AIChE

Modeling the Crystallization of Proteins and Small Organic Molecules in Nanoliter Drops

Richard D. Dombrowski and James D. Litster
Div. of Chemical Engineering, Particle and Systems Design Centre, University of Queensland, Brisbane, QLD 4072, Australia

Norman J. Wagner
Dept. of Chemical Engineering, Center for Molecular and Engineering Thermodynamics, University of Delaware, Newark, DE 19716

Yinghe He
School of Engineering, James Cook University, Townsville, QLD 4811, Australia

DOI 10.1002/aic.12001
Published online September 9, 2009 in Wiley InterScience (www.interscience.wiley.com)

Drop-based crystallization techniques are used to achieve a high degree of control over crystallization conditions in order to grow high-quality protein crystals for X-ray diffraction or to produce organic crystals with well-controlled size distributions. Simultaneous crystal growth and stochastic nucleation makes it difficult to predict the number and size of crystals that will be produced in a drop-based crystallization process. A mathematical model of crystallization in drops is developed using a Monte Carlo method. The model incorporates key phenomena in drop-based crystallization, including stochastic primary nucleation and growth rate dispersion (GRD) and can predict distributions of the number of crystals per drop and full crystal size distributions (CSD). Key dimensionless parameters are identified to quickly screen for crystallization conditions that are expected to yield a high fraction of drops containing one crystal and a narrow CSD. Using literature correlations for the solubilities, growth, and nucleation rates of lactose and lysozyme, the model is able to predict the experimentally observed crystallization behavior over a wide range of conditions. Model-based strategies for use in the design and optimization of a drop-based crystallization process for producing crystals of well-controlled CSD are identified. © 2009 American Institute of Chemical Engineers *AIChE J,* 56: 79–91, 2010
Keywords: crystallization, nucleation, crystal growth, mathematical modeling, particle technology

Introduction

Emulsion drops have been shown to be useful as microreactors for the production of particulate materials with controlled size, shape, or polymorph.[1,2] A number of new drug-delivery technologies are dependent upon the ability to manufacture particles of well-controlled size. For example, pulmonary drug delivery devices require particles between 1 and 6 μm for optimal delivery and retention in the

Correspondence concerning this article should be addressed to R. D. Dombrowski at rdombro@udel.edu
Current address of R.D. Dombrowski Department of Chemical Engineering, University of Delaware, Newark, DE 19716.

respiratory tract.[3] Controlled-release drug formulations with the desired temporal release profile in the body can be prepared by using crystals/particles having a well-defined crystal size distribution (CSD).[4]

Protein crystallization is often investigated by studying crystallization in nearly monodisperse drops, using hanging or sitting drops[5] or drops in microfluidic channels.[6] The goal of these crystallization studies is to screen the large parameter space in order to find a set of conditions that yield a large, single crystal in the drop. The crystal is then harvested and the protein structure is determined using X-ray diffraction. Currently, the crystallization step is a major limitation in the process of going from protein isolation and purification to structure determination. Improved understanding of the phenomena that control the number and size of crystals formed in drops may accelerate the process of creating large, single crystals in drops and may enable more rapid breakthroughs in biotechnology fields.

Recently, an emulsion-based crystallization process has been demonstrated as a means for producing large populations of crystals of controlled, narrow size distribution.[7] A schematic illustration of the emulsion-based crystallization is shown in Figure 1. The mother liquor is distributed as uniform drops that travel down a tubular crystallizer. The geometry and surface properties of the tubular crystallizer prevent drop coalescence, eliminating the need for a stabilizing surfactant.[8] The lack of interaction and/or coalescence of the monodisperse drops means that each drop contains the same mass of solute available to crystallize, thus the maximum crystal size is identical for each drop. Under optimal conditions, one crystal is formed in each drop and a narrow CSD near the mass balance limited size is produced.

Crystallization in drops is a complex system where nucleation, growth and Ostwald ripening may occur. Following nucleation of the first crystal, the drop remains in a supersaturated state during growth of the initial crystal. During this growth time, it is possible that more crystals may nucleate due to the supersaturated conditions. The nucleation and growth of multiple crystals in drops is undesirable and will lead to a crystal size smaller than the mass balance limited size and a significantly broader CSD. The number and size(s) of the crystals produced in the drops depends on a large number of factors, including temperature, initial concentration, drop size, the concentration dependences of nucleation and growth rates, growth rate dispersion, pH, and salt concentration. The processes that determine the CSD from crystallization in drops, in particular nucleation and growth rates, exhibit wide variation across different solvent/solute systems. Thus, the main challenge when using the drop-based crystallization process is to rapidly identify crystallization conditions that will lead to the production of only one crystal per drop for the material of interest. A trial-and-error experimental approach to finding optimal conditions is inefficient and time consuming due to the large number of variables that determine crystal growth and nucleation rates. Model-based screening of the vast parameter space can be used to quickly identify parameter ranges that are likely to produce one crystal per drop and narrow CSD.

In addition to stochastic nucleation, the random nature of growth rate dispersion (GRD) should be accounted for when modeling the crystallization of a solute that exhibits significant GRD. GRD is a phenomenon where crystals of the same material, exposed to the same growth conditions will have a distribution of growth rates about the mean. A number of materials show GRD, including organic[9,10] and inorganic[11,12] materials. Since the crystal growth rate directly impacts how rapidly the supersaturation is depleted in a drop, the variation in growth rates due to GRD can lead to additional variability in the number of crystals that nucleate in each drop.

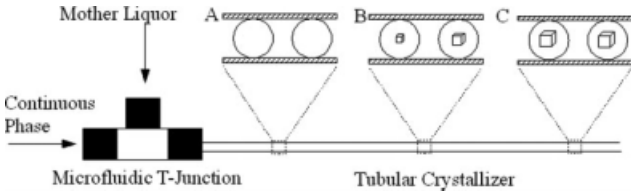

Figure 1. Schematic of the microfluidic drop-based crystallization process.

A number of previous experimental and numerical studies of crystallization in emulsions have considered an emulsified melt as the crystallizing phase.[13,14] In melt emulsion crystallization each drop typically forms one particle, meaning that a narrow drop size distribution will lead to a narrow particle size distribution.[15,16] In the case of solution crystallization in drops, experiments have shown that one drop does not always produce one crystal.[7,17] For solution crystallization, the crystal size distribution will depend on the initial drop size distribution, along with factors such as the distribution of the number of crystals per drop, the extent of GRD shown by the material and the distribution of nucleation times within each drop. Previous models of protein crystals in hanging drops predict the mean number of crystals and mean crystal size but neglect the stochastic aspects of nucleation and growth rate dispersion.[18] A model that incorporates these stochastic phenomena is needed to accurately capture the distribution of the number of crystals per drop and/or crystal size distributions.

This article presents a model of crystallization in drops that uses Monte Carlo methods to model the effects of growth rate dispersion and stochastic primary nucleation. The current model is not limited by the mononuclear assumption of the previous models of emulsion crystallization and thus can predict full distributions of the number and size of crystals in the drops. Development of the model provides insight into the key dimensionless parameters that control the crystallization behavior, thereby allowing the effects of multiple crystallization process variables to be condensed into a single parameter that may be used to predict the outcome of a drop-based crystallization process. The model predictions and choice of dimensionless parameters are validated using experimental crystallization results for lactose and lysozyme. Strategies for optimizing the drop-based crystallization process are developed from the model formulation and validation.

Model Development

Solubility, growth, and nucleation correlations

The major factor that determines the results of any crystallization process is the concentration of solute in the mother

liquor (i.e., supersaturation). Crystal growth and nucleation rates are both typically strong functions of supersaturation. In stirred-tank crystallizers, the macroscopic supersaturation may be considered to be uniform throughout the vessel, but micromixing has a significant and unpredictable effect on nucleation. Unlike a stirred-vessel crystallizer, each drop in the drop-based crystallizer may have a different supersaturation at a particular time during crystallization, but each drop can be considered truly well-mixed. The concentration of solute remaining in solution in a drop containing i crystals, each with size x_i, is calculated from the mass balance on a drop:

$$C(\mathbf{x}) = \left(\frac{100}{m_{\mathrm{H_2O}}}\right)\left(m_{\mathrm{S0}} - \alpha_{\mathrm{V}}\rho_{\mathrm{C}}\sum_i x_i^3\right) \tag{1}$$

where $C(\mathbf{x})$ is the concentration expressed in grams of solute per 100 grams of water (g/100g), α_{V} is the volume shape factor, ρ_{C} is the crystal density and $m_{\mathrm{H_2O}}$ and m_{S0} are the initial masses of water and solute in the drop, respectively. It is assumed that (a) there is no transport of either solute or solvent through the continuous phase or exchange of material between adjacent drops in the tubular crystallizer; and (b) there are no solvent inclusions in the crystal, although water of crystallization is allowed.

Equation 1 and solubility data or a suitable solubility correlation can be used to calculate the level of supersaturation in the drop. The relative supersaturation (dimensionless) is:

$$S(\mathbf{x}) = \frac{C(\mathbf{x})}{C_{\mathrm{S}}} \tag{2}$$

The absolute supersaturation (concentration units) is defined as:

$$\Delta C(\mathbf{x}) = C(\mathbf{x}) - C_{\mathrm{S}} \tag{3}$$

where C_{S} is the solubility concentration which is a function of the state variables including temperature, pH or salt concentration.

Nucleation rates in drops are modeled using classical nucleation theory[19]

$$J(\mathbf{x}) = A\exp\left(-\frac{16\pi\gamma^3 V_{\mathrm{m}}^2}{3k^3T^3\ln[S(\mathbf{x})]^2}\right) \tag{4}$$

where A is a nucleation rate constant, γ is the crystal-solution interfacial tension, V_{m} is the solute molecular volume, k is Boltzmann's constant and T is the absolute temperature. The pre-exponential factor is assumed to have Arrhenius temperature dependence

$$A(T) = A_0\exp\left(-\frac{E_{\mathrm{A}}}{kT}\right) \tag{5}$$

In the model, it is assumed that an existing crystal does not catalyze nucleation of further crystals and the nucleation rate may be described by Eqs. 4 and 5 for any number of crystals present in the drop. Secondary nucleation due to attrition is expected to be negligible in the quiescent drops. Growth of existing crystals will have an effect on the nucleation rate due to the depletion of the supersaturation in the drop.

Experimentally measured crystal growth rates are often correlated using a power-law expression:

$$G(\mathbf{x}) = k_{\mathrm{G}}\Delta C(\mathbf{x})^a \tag{6}$$

where $G(\mathbf{x})$ is the mean growth rate in a system that exhibits GRD. Experimental values for the rate exponent a are typically between 1 or 2, although higher values have been observed for some materials and/or individual crystal faces.[20] In the modeling presented in this article, $a = 2$, corresponding to surface-integration controlled growth.[21] To model GRD, each crystal is randomly assigned a constant growth rate multiplier when that crystal nucleates and the growth rate equation becomes:

$$G(\mathbf{x}) = k_{\mathrm{G}}k_{\mathrm{GRD}}(\mathbf{x})\Delta C(\mathbf{x})^a \tag{7}$$

The relative growth rate multiplier, k_{GRD}, is different for each crystal and is drawn from a log-normal distribution of growth rates with the width of the distribution characterized by $\mathrm{CV_G}$, the coefficient of variation of growth rates.

Dimensionless growth and nucleation times

The growth and nucleation rates of different materials vary widely. To develop a sufficiently general model and to highlight the dominant relationships, it is useful to define characteristic time scales for growth and nucleation and corresponding dimensionless quantities. The characteristic nucleation time for a given material and set of conditions can be considered as the mean time required for one crystal nucleus to form in a drop of volume V:

$$t_{\mathrm{Nucl}} = 1/JV \tag{8}$$

A characteristic time for growth can be calculated as the ratio of the maximum crystal size and the initial linear crystal growth rate:

$$t_{\mathrm{Growth}} = \frac{L_{\mathrm{max}}}{G_0} \tag{9}$$

L_{max} is found by setting the right hand side of Eq. 1 equal to C_{S} and solving for $\mathbf{x}$ when only one crystal is present in the drop. G_0 is calculated from Eq. 6 with $\mathbf{x} = 0$.

Dimensionless nucleation and growth times are then defined as the ratio of the elapsed process time t to the characteristic nucleation and growth times as defined earlier:

$$\tau_{\mathrm{N}} = \frac{t}{t_{\mathrm{Nuc}}} = \frac{t}{\frac{1}{JV}} = JVt \qquad \tau_{\mathrm{G}} = \frac{t}{t_{\mathrm{Growth}}} \tag{10}$$

The dimensionless crystal size is defined as:

$$L_i^* = \frac{x_i}{L_{\mathrm{max}}} \tag{11}$$

Limiting cases

A model of crystallization in drops should predict both the CSD and the distribution of the number of crystals per drop. Analytical solutions for the fraction of drops containing zero, one, two, or more crystals as a function of t can be obtained for some limiting cases. The first limiting case is when crystal growth is extremely slow and $t_{\text{Growth}} \rightarrow \infty$. For crystallization at constant temperature, pH, salt concentration, etc., the nucleation rate is constant throughout the process and the number of drops containing j crystals at any time can be calculated from a Poisson distribution.[22]

$$N_j(t) = N_T \frac{(JVt)^j}{j!} \exp(-JVt) = N_T \frac{\tau_N^j}{j!} \exp(-\tau_N) \tag{12}$$

where N_T is the total number of drops and τ_N is the dimensionless nucleation time, as defined in Eq. 10. For $j = 0$, an exponential decay in the number of drops with no crystals is obtained:

$$N_0(\tau_N) = N_T \exp(-\tau_N) \tag{13}$$

Optimization of the emulsion crystallization process aims to maximize the fraction of drops containing one crystal. All of the drops with two or more crystals can be lumped together as multiple crystal drops and the equations describing Poisson-type crystallization behavior become

$$N_1(\tau_N) = N_T \tau_N \exp(-\tau_N) \tag{14}$$

$$N_m(\tau_N) = N_T - N_0(\tau_N) - N_1(\tau_N) \tag{15}$$

From Eq. 14 it can be shown that the maximum attainable fraction of drops with one crystal for a system following Poisson behavior, for any value of JV, is 0.37. Thus, it is not possible to obtain a large fraction of drops containing only one crystal and a very narrow CSD for a system that exhibits Poisson crystallization behavior.

The other limiting case is the rapid growth limit where G_0 is large and $t_{\text{Growth}} \rightarrow 0$. With rapid growth the supersaturation in a drop is instantly depleted once the first crystal nucleates, thereby preventing formation of a second crystal. The number of empty drops follows the same exponential decay from Eq. 13. The number of drops with one crystal becomes:

$$N_1(\tau_N) = N_T(1 - \exp(-\tau_N)) \tag{16}$$

The Poisson and rapid growth models can predict the distribution of the number of crystals per drop, but offer only general, qualitative predictions about the crystal size distribution. Clearly, more complex models are required to predict full crystal size distributions for emulsion crystallization with real crystal growth rates. The limiting cases presented in this section provide a basis for testing more complicated models to ensure accuracy and consistency and provide a foundation for interpreting experimental results.

Monte Carlo model development

Analytical solutions for the limiting cases presented earlier are possible because of the assumption of zero or instantaneous growth, which eliminates the need to consider the dynamics of nucleation and growth within a drop. For more general conditions, the change in supersaturation (i.e., nucleation and growth rates) as crystals grow in drops must be considered. Primary nucleation and GRD both represent stochastic phenomena, thus a Monte Carlo type model that explicitly simulates these random processes is a logical choice for developing a mathematical model of crystallization in drops. Simulations using the Monte Carlo method are also computationally efficient relative to other methods. A partial differential equation based simulation approach, such as the population balance, becomes extremely computationally expensive with realistic growth rate distributions and more than two or three crystals per drop. A schematic depiction of the Monte Carlo method is shown in Figure 2.

After setting the initial simulation conditions, Eq. 17 is used to calculate the probability of a crystal nucleating in the chosen time step, Δt:

$$P_{\text{Nuc}}(\mathbf{x}, t) = 1 - \exp(-J(\mathbf{x}, t)V\Delta t) \tag{17}$$

where J is the nucleation rate as defined in Eq. 4. The time dependence of J arises from its dependence on temperature, which is allowed to vary with time during crystallization. For the development and validation of the model it is assumed that the crystallization process is isothermal.

To model stochastic nucleation a random number is drawn from a uniform distribution between 0 and 1. If the random number is less than P_{Nuc} a new crystal nucleus is formed in the model. Immediately following a successful nucleation draw, a second random number is drawn from a growth rate distribution to assign the new crystal's growth rate relative to the mean to simulate GRD. The new crystal and any existing crystals grow and new S, G, and J are calculated from the mass balance and Eqs. 4 and 7 for growth and nucleation rates, respectively. If the supersaturation is depleted to below the nucleation threshold due to the growth of existing crystals, J is automatically set to 0 to prevent further nucleation. The simulation loops until the total simulation time is reached and the final CSD and CSD statistics are calculated. The spread of the CSD is represented by the coefficient of variation (CV):

$$\text{CV} = \frac{\sigma}{\mu_{10}} \tag{18}$$

where σ is the arithmetic standard deviation and μ_{10} is the number mean crystal size.

Most of the model parameters are determined by the physical system being modeled (e.g., crystal density, shape factor, growth rate constant) and may be measured or obtained from literature. The model time step is an important user-defined parameter in the Monte Carlo simulation. The time step is directly proportional to the number of times the main simulation loop is run and therefore determines the computational expense of the simulation. In the Monte Carlo model, the growth rate is constant over a single time step. If a very coarse time step is chosen, the simulated crystals can grow to the maximum size within the same time interval in which they nucleated, potentially leading to over prediction of the fraction of drops with one crystal or crystals larger than

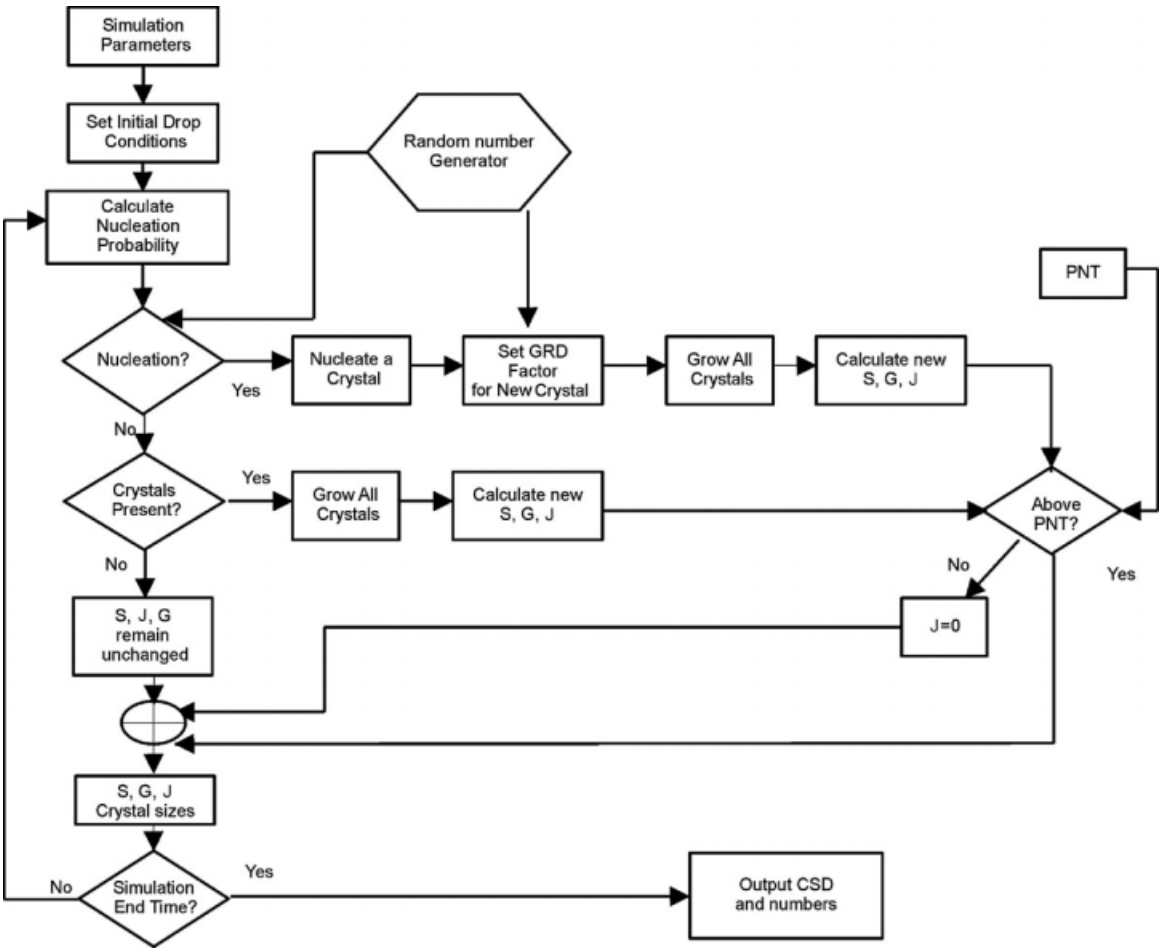

Figure 2. Schematic of Monte Carlo model.

L_{max}, a physically unrealistic result. A time step of 0.02 t_{Nuc} resulted in less than a 2% difference between simulation and analytical solution for both the Poisson and rapid growth limits. Therefore, we use this value throughout the work presented in the next section.

Results and Discussion

Model testing and sensitivity analysis

Lactose, an organic molecule which exhibits significant GRD,[23] is a convenient test case for the model. The physical parameters and the crystallization conditions for the initial lactose crystallization simulations are listed in Table 1.

The growth constant k_G was multiplied by 10^2 or divided by 10^6 to simulate the rapid growth or Poisson limit, respectively. Ten thousand drops were simulated for $0 < \tau_N < 2.2$ with a time step of 0.02 t_{Nuc}. Model predictions for the number of crystals per drop are compared with analytical solutions in Figure 3. In both limits the agreement between model and analytical solution is excellent, with $R^2 > 0.99$.

To explore the effects of changing the relative nucleation and growth rates, the rate constants (A_0 and k_G) were multiplied by factors from e^{-4} to e^4. Altering any parameter appearing in Eqs. 4 and 6 will change the respective rates of growth or nucleation, but the constants A_0 and k_G provide the most direct means to manipulate the relative rates. The particular choice of the manipulated variables is not as important as the resulting relative rates of nucleation and growth, which are characterized by the parameter $\ln(\tau_G/\tau_N)$.

The model predicted fractions of drops with one and multiple crystals for different $\ln(\tau_G/\tau_N)$ are shown in Figure 4. The fraction of empty drops follows a simple exponential decay with increasing τ_N regardless of the growth rate and is not shown. The model predictions converge to the limiting analytical solutions for $\ln(\tau_G/\tau_N) < -2$ (Poisson limit) and

Table 1. Crystallization Parameters for Initial Simulations

Parameter	Value
d_{drop}	150 μm
C_0	76 g/100g
C_S	19 g/100g*
T	293 K
γ	5.9 mN m†
ρ_C	1540 kg m^{-3}
V_m	3.88×10^{-28} m^{-3}
A_0	5.4×10^{27} nuclei m^{-3} s$^{-1\dagger}$
E_A	108 kJ mol$^{-1\dagger}$
k_G	1.13×10^{-13} $(T - 273.15)$ m s^{-1} (g/100g)$^{-2\dagger}$
CV_G	0.4*

*See Ref. 24.
†See Ref. 7.

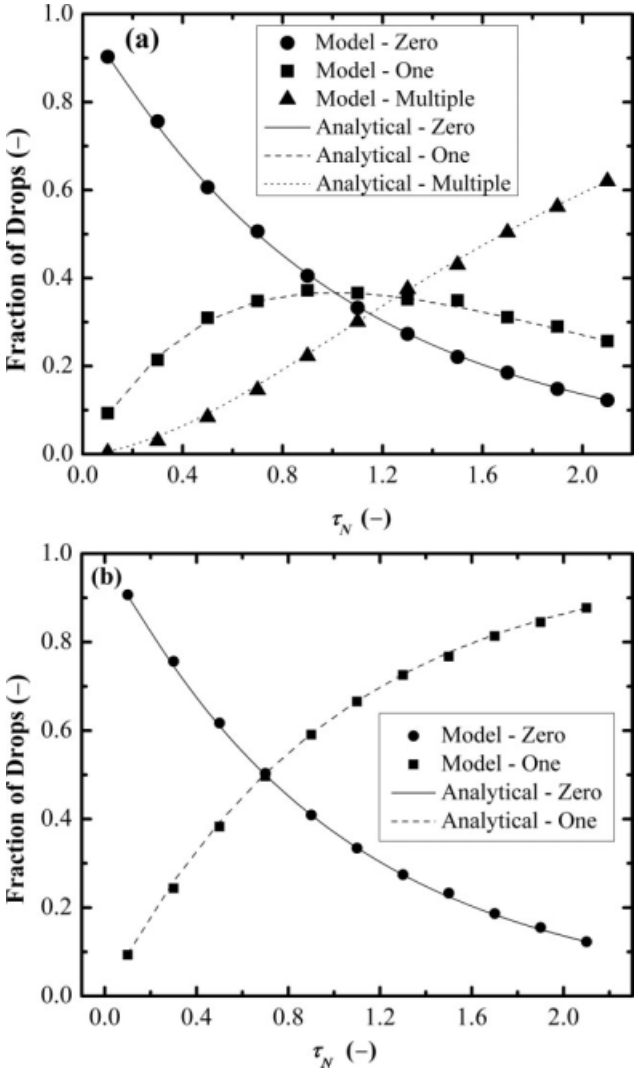

Figure 3. Monte Carlo model predicted fractions of drops with zero, one and multiple crystals in the (a) Poisson limit (b) Rapid growth limit.

$\ln(\tau_G/\tau_N) > 3$ (rapid growth limit). The mean and CV of the total crystal size distribution corresponding to each relative growth and nucleation rate are shown in Figure 5.

From the distributions of the number of crystals per drop in Figure 4 and the CSD statistics in Figure 5 it is evident that fast growth relative to nucleation produces the highest fraction of drops with one crystal and narrowest CSD. Faster growth also narrows the CSD by rapidly reducing the difference in size between large single crystals that nucleated early in the process and those crystals that nucleated later in the process and have not had enough time to grow to a size near $L^* = 1$.

Lactose crystallization in drops—model validation

Lactose is an organic molecule that exhibits GRD and has previously been crystallized in drops.[7] The physical properties and correlations for growth and nucleation are available from the literature, as listed in Table 1. Therefore, there are no additional fitting parameters needed to model lactose crystallization in drops for comparison with experimental results. Experimentally, lactose showed an apparent Poisson type behavior when crystallized in 300 μm drops between 293 K and 313 K.[7] As shown earlier, the parameter $\ln(\tau_G/\tau_N)$ correlates with the expected crystallization behavior. Equations 4–9 and the nucleation and growth correlations from Dombrowski et al. were used to calculate τ_G and τ_N and the estimated value of $\ln(\tau_G/\tau_N)$ from the initial supersaturation ratio in each experiment.[7] The parameter $\ln(\tau_G/\tau_N)$ ranged from -0.6 to 1.2 in the crystallization experiments at 293 K, from -0.7 to 2.1 at 303 K and from 1.4 to 3.5 at 313 K. Based solely on the calculated $\ln(\tau_G/\tau_N)$ for the conditions tested, lactose crystallization is expected to be intermediate between the Poisson and rapid growth limits.

At the lower range of initial supersaturations (e.g., $S_0 <$ 3.1 at 293 K) the experimental results and model predictions for the distribution of the number of crystals per drop show good agreement, as shown in Figure 6. The model accurately

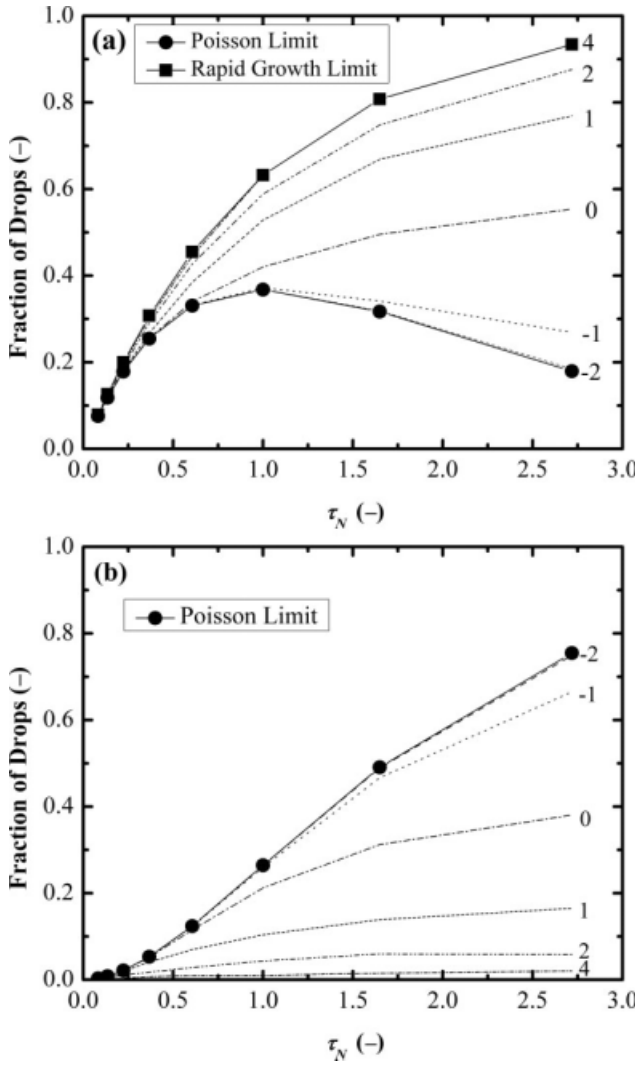

Figure 4. Model predicted fractions of drops with (a) one crystal, (b) multiple crystals.

The value of $\ln(\tau_G/\tau_N)$ is listed next to each curve.

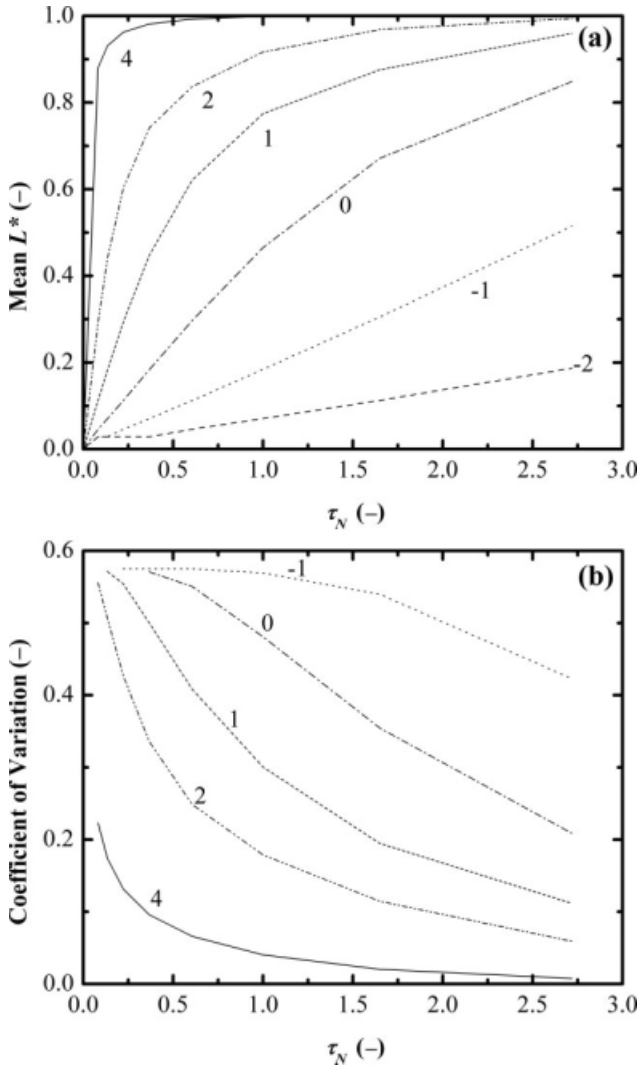

Figure 5. Model predicted (a) dimensionless mean crystal size and (b) coefficient of variation.

The value of $\ln(\tau_G/\tau_N)$ is listed next to each curve.

predicts the fraction of empty drops ($R^2 = 0.89$), but does not completely capture the fraction of single or multiple crystal drops over the entire supersaturation range ($R^2 = 0.28$). The main discrepancy between the model and experiment is that the model predicts a slower increase in the fraction of multiple crystal drops than is seen experimentally as S_0 is increased. The difference may simply stem from uncertainty in the experimentally determined growth or nucleation correlations. When either growth or nucleation strongly dominates ($|\ln(\tau_G/\tau_N)| > 2$) the predicted fractions of single or multiple crystal drops is less sensitive to errors in experimentally determined growth and nucleation rates. Figure 7 illustrates the enhanced sensitivity to the experimentally determined parameters when growth and nucleation are approximately balanced. When $\ln(\tau_G/\tau_N) = 0$, changing the growth rate constant by a factor of two can swing the model prediction from nearly Poisson behavior to intermediate rapid growth behavior (Figure 7a). When $\ln(\tau_G/\tau_N) = 2$ initially, a similar change in the growth rate constant causes a smaller change in the fraction of drops with one crystal and the system remains close to the rapid growth limit (Figure 7b). For the case of crystallization at 293 K in 300 μm drops shown in Figure 6, $\ln(\tau_G/\tau_N) = 0$ at $S_0 = 3.15$.

There are two additional phenomena that are not included in the model that may be responsible for some of the observed discrepancy. Heterogeneous nucleation due to particulate impurities in some drops would be expected to increase the fraction of drops with multiple crystals. Another possibility is that the first crystal in a drop may catalyze the secondary nucleation of additional crystals. Either of these phenomena would act to increase the fraction of drops containing more than one crystal. Both phenomena represent a lowering of the energy barrier to nucleation (γ in Eq. 4) and the effects would be expected to increase rapidly with increasing S; consistent with the experimentally observed precipitous drop in the fraction of single crystal drops and corresponding rapid increase in multiple crystal drops at 293 K and $S_0 = 3.15$. However, there are no experimentally measured correlations to predict the rates of heterogeneous or secondary nucleation of lactose in the drops and attempting to model these phenomena would simply amount to forcing the model to fit the data by introducing additional parameters.

Prediction of the number of crystals per drop can be used to infer some qualitative conclusions about the product CSD, but the explicit incorporation of stochastic nucleation and GRD in the Monte Carlo model means that the full CSD may be predicted. A comparison of the model predicted and experimental CSD obtained from 24 h crystallization in 300 μm drops at 293 K with $S_0 = 3.0$ is shown in Figure 8a. The component CSDs in single and multiple crystal drops are shown in Figure 8b. The key CSD statistics are listed in Table 2. The model predicts the mean crystal size within 13% for the total CSD as well as the component CSDs. However, the model overestimates the width of the distribution, predicting a broader distribution than is observed

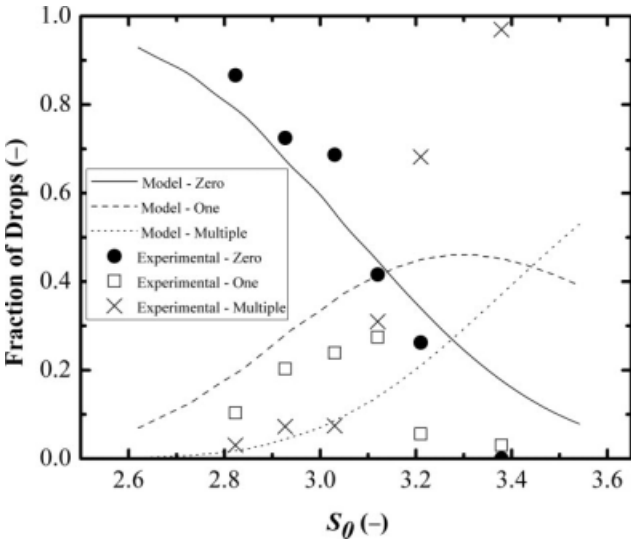

Figure 6. Experimental and model predicted number of lactose crystals per drop produced after 24 h and 293 K in 300 μm drops.

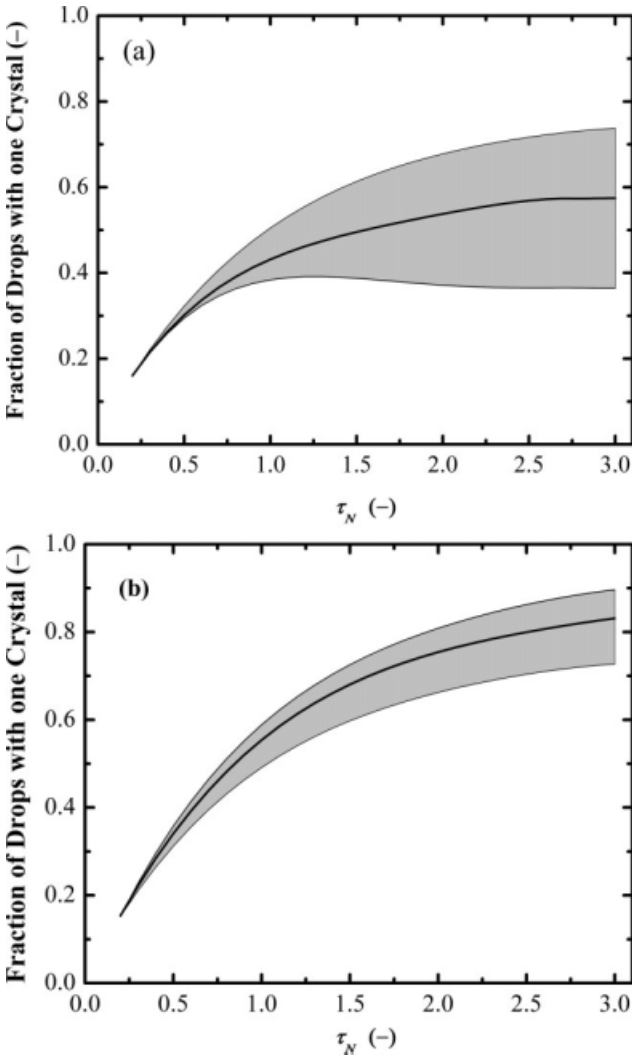

Figure 7. Model sensitivity to uncertainty in experimentally determined parameters.

The shaded areas indicate the range of model predictions that result from changing k_G by up to a factor of 2 for (a) $\ln(\tau_G/\tau_N) = 0$ (b) $\ln(\tau_G/\tau_N) = 2$.

experimentally. Heterogeneous nucleation in the experimental results may skew the distribution towards larger crystal sizes by increasing the number of crystals that nucleate near $t = 0$, thereby increasing the number of crystals that are able to grow during the entire experimental time. The slight discrepancy in the model and experimental CSDs does not alter the main conclusions that may be drawn from both the experimental and model results: crystals do not have enough time to grow to $L^* \approx 1$, thus the particular set of conditions does not take advantage of the benefits of confined crystallization and is not expected to produce a narrow CSD.

A crystallization simulation was also run for 24 h crystallization in 300 μm drops at 313 K with $S_0 = 2.3$. At this set of crystallization conditions $\ln(\tau_G/\tau_N) = 3.5$, the highest of the published lactose crystallization experiments.[7] It is expected that these conditions will better utilize the growth-limiting effects of drop-based crystallization than the experiment at 293 K and $S_0 = 3.0$. The total and component CSDs for the experiment at 313 K are shown in Figures 8c and d, respectively. In both the model and experimental results an upturn is seen in the CSD at larger crystal sizes, indicating that some crystals have grown to nearly $L^* = 1$, such that additional time will allow slow-growing or late nucleating crystals in other drops to "catch up," leading to a narrower CSD.

Considering the complexity of the system and the uncertainty in growth and nucleation correlations, the Monte Carlo model accurately captures the important behavior in the microfluidic crystallizer. The model provides insight into whether a particular set of conditions will be able to take advantage of the size-limiting effects of crystallization in drops. At conditions that utilize the growth-limiting effects of confined crystallization in drops to the fullest, such as with fast growth rates, the agreement between the model predictions and experimental results is excellent.

Crystallization of lysozyme in drops—validation of model and use of $\ln(\tau_G/\tau_N)$ as design parameter

Much of the interest in drop-based crystallization focuses on crystallization of proteins. Lysozyme is by far the most crystallized protein and is often selected as a "model protein" in crystallization experiments. The large number of lysozyme crystallization studies means that the rate parameters required for modeling crystallization in drops can be obtained from the literature and are relatively reliable. Additionally, heterogeneous nucleation in drop-based lysozyme crystallization has been characterized in some studies[17] or nearly eliminated by combining the protein and precipitant solutions as the drops are formed,[25] thereby reducing a major source of uncertainty that was present in the lactose crystallization experiments. As it will be shown shortly, the previous studies of lysozyme crystallization in drops have used conditions that would be expected to produce behavior that spans the spectrum from the rapid growth limit to the Poisson limit. The broad range of crystallization conditions provides the basis for validating the parameter $\ln(\tau_G/\tau_N)$ as a means for rapidly predicting crystallization behavior.

Lysozyme nucleation rates measured in previous studies rates have been correlated using a slightly modified form of Eq. 4[26]:

$$J(\mathbf{x}) = \mathrm{AC}(\mathbf{x}) \exp\left(\frac{-B}{\ln[S(\mathbf{x})]^2}\right) \tag{19}$$

with $A = 17.4$ nuclei m^{-3} s^{-1} (mg mL)$^{-1}$ and $B = 51.33$. Lysozyme crystal growth rates have been extensively studied over a wide range of crystallization conditions.[27–29] Cherdrungsi correlated the measured growth rates of lysozyme crystals, in μm s^{-1}, from the various studies[30]:

$$G = 3.5 \times 10^{-4}(\sigma - b)^{1.5} \exp\left(\frac{T - 295\mathrm{K}}{9\mathrm{K}}\right) \times \exp\left(\frac{5\%\mathrm{w/v} - \%\mathrm{NaCl}}{4\%\mathrm{w/v}}\right) \tag{20}$$

where $\sigma = S - 1$, b is a correction for the different solubilities used by different authors, (taken as 0 in the model) and %NaCl

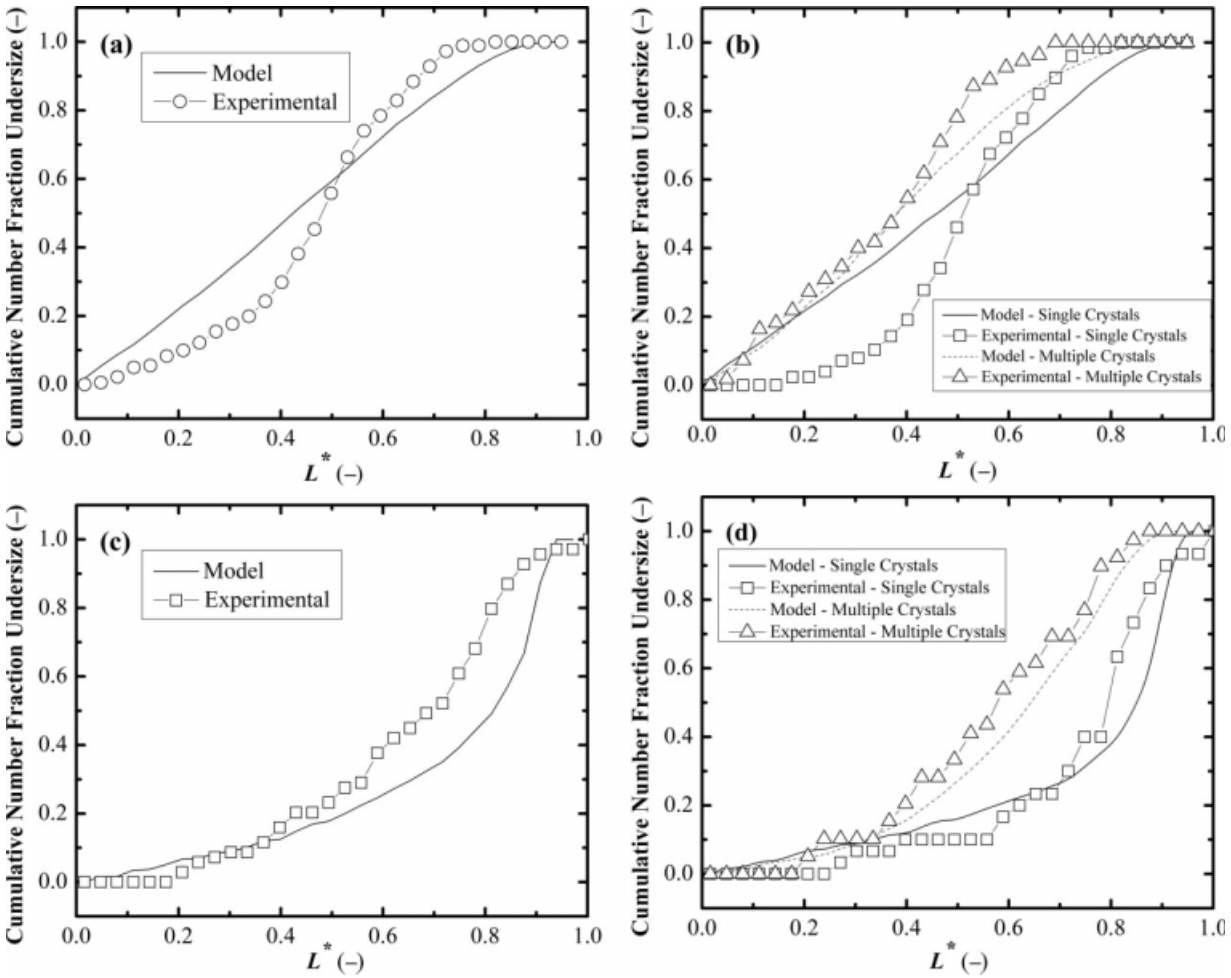

Figure 8. CSDs from 24 h lactose crystallization in 300 μm drops (a) full CSD at 293 K, S_0 = 3.0; (b) component CSDs at 293 K, S_0= 3.0; (c) full CSD at 313 K, S_0 = 2.3; (d) component CSDs at 313 K, S_0 = 2.3.

is the salt concentration in % w/v. The remaining physical parameters of relevance for modeling lysozyme crystallization are listed in Table 3. As was the case with the modeling of lactose crystallization, there are no additional fitting parameters used in the modeling of lysozyme crystallization.

Crystallization of lysozyme in drops—$ln(\tau_G/\tau_N) < 0$

Galkin and Vekilov used a two-step temperature profile to study the nucleation of lysozyme in 0.7 μL ($d \approx 1.1$ mm) drops.[17] Nucleation rates were extracted from the distributions of the number of crystals per drop using a Poisson model. The authors do not report size distributions, but the distributions of the number of crystals per drop can be used to test the Monte Carlo model presented earlier. A comparison of the model predicted and experimentally measured mean number of crystals formed when $\ln(\tau_G/\tau_N) = -1.5$ (285.7 K, 2.5 wt % NaCl and 55.5 mg mL^{-1} initial lysozyme concentration) is shown in Figure 9. The value of $\ln(\tau_G/\tau_N)$ at these conditions indicates that the crystallization behavior would be expected to be close to the Poisson limit (Refer to Figure 4). The nonzero y-intercept in the experimental data shown in Figure 9 is due to heterogeneous nucleation, which the model does not capture. After adjusting for the effects of heterogeneous nucleation by subtracting the intercept, the model predicted and experimentally observed number of homogeneously nucleated crystals show excellent agreement ($R^2 = 0.94$).

Table 2. Experimental and Model Predicted CSD and Component CSD Statistics for Lactose Crystallization

	All Crystals		Single Crystals		Multiple Crystals	
	Mean (μm)	CV	Mean (μm)	CV	Mean (μm)	CV
Exptl. 20°C	148	0.35	163	0.26	114	0.48
Model 20°C	135	0.55	143	0.54	121	0.55
Exptl. 40°C	207	0.31	237	0.24	183	0.33
Model 40°C	223	0.35	232	0.34	191	0.35

Table 3. Crystallization Parameters Used in the Simulation of Lysozyme Crystallization

Physical Parameter	Value
Molecular Weight	14,600 g mol^{-1}*
ρ_C	1230 kg m^{-3}†
V_m	3×10^{-26} m^3‡

*See Ref. 31.
†See Ref. 32.
‡See Ref. 16.

Figure 10 shows a comparison of the model predicted and experimental distribution of the number of crystals after 1 h in 1.1-mm diameter drops with $\ln(\tau_G/\tau_N) = -2.9$ (285.7 K and 2.5 wt % NaCl, initial lysozyme concentration of 69.5 mg mL^{-1},) as measured by Galkin and Vekilov. The model confirms that the experimentally observed Poisson-like behavior is to be expected for the particular crystallization conditions. The model predicts that the Poisson process would be "farther along" than experimentally observed after 1 h, however the difference is well within the uncertainty expected from the use of the experimentally determined nucleation correlation. The results of the experimental study of lysozyme nucleation agree with the conclusions from the theoretical development of the model: a set of crystallization conditions yielding a large, negative value of $\ln(\tau_G/\tau_N)$ will not produce a high fraction of drops with one crystal and a narrow CSD.

Crystallization of lysozyme in drops—$\ln(\tau_G/\tau_N) > 0$

The lysozyme concentration in the 1.1-mm diameter drops used by Galkin and Vekilov was mostly unaffected by the growth of crystals at small crystallization times. In smaller drops the growth of crystals will have a substantial effect on the lysozyme concentration remaining in a drop. Lysozyme crystallization in 150 μm drops was investigated using a drop-based microfluidic crystallizer as in Dombrowski et al.[7] Lysozyme was crystallized in 150 μm drops with $\ln(\tau_G/\tau_N) = 8.4$–3.8 (277 K, pH = 4.1 and 4 wt % NaCl, with initial lysozyme concentrations from 7 to 21 mg mL^{-1}, respectively). In the experiment with an initial concentration of 20 mg mL^{-1} the microfluidic crystallizer was slightly modified to mix the protein and salt solutions immediately before drop formation, similar to the approach used in previous protein crystallization studies.[31] The measured and model predicted fractions of drops with zero and one crystal after 72 h are shown in Figure 11. The model accurately predicts the experimentally observed behavior, namely that lysozyme exhibits rapid growth-type behavior when crystallized in 150 μm drops and conditions that yield a value of $\ln(\tau_G/\tau_N) > 2$.

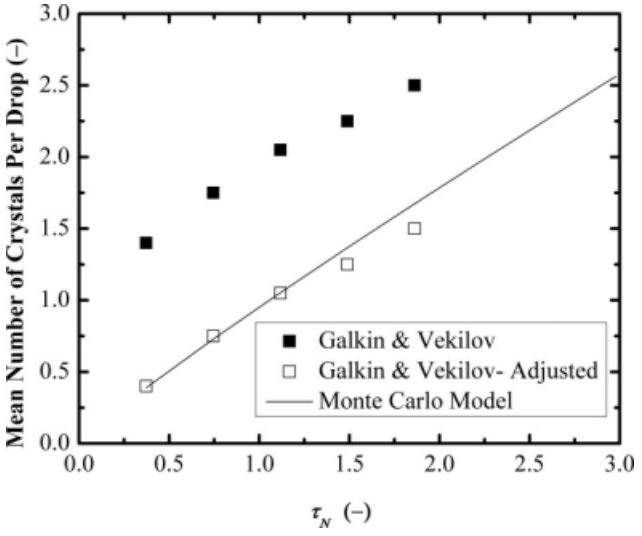

Figure 9. Comparison of the mean number of lysozyme crystals per drop in 1.1-mm drops observed experimentally[17] and predicted by the Monte Carlo model.

Experimental results are adjusted to account for heterogeneous nucleation using the same method as Galkin and Vekilov.

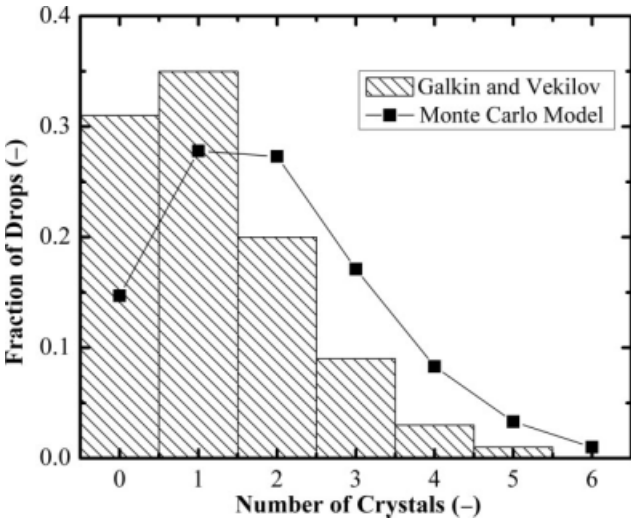

Figure 10. Distribution of the number of lysozyme crystals per drop observed experimentally[17] and predicted by the Monte Carlo model.

The difference in crystallization results in the 150 μm drops and the 1.1 mm drops is explained by considering the supersaturation vs. time profile following nucleation of the first crystal, shown in Figure 12. The supersaturation is rapidly depleted in the 150 μm drops due to growth of the first crystal; thus, nucleation of a second crystal becomes highly improbable. The crystallization behavior approaches the rapid growth limit and nearly all of the drops that have nucleated contain only one crystal. In contrast, the supersaturation remains above 99% of the initial value up to $\tau_N \approx 4$ in the 1.1-mm drops. Even calculating the nucleation rate using the assumption that $S/S_0 = 0.99$ up to $\tau_N = 4$ suggests a 97% probability of nucleating a second crystal before crystal growth would reduce the supersaturation below 99% of the original value.

Model-Based Process Design

A drop-based process for producing crystals of controlled size should yield a high fraction of drops containing one crystal that has grown to $L^* \approx 1$. This result is achieved when a drop-based crystallizer is operated at conditions that

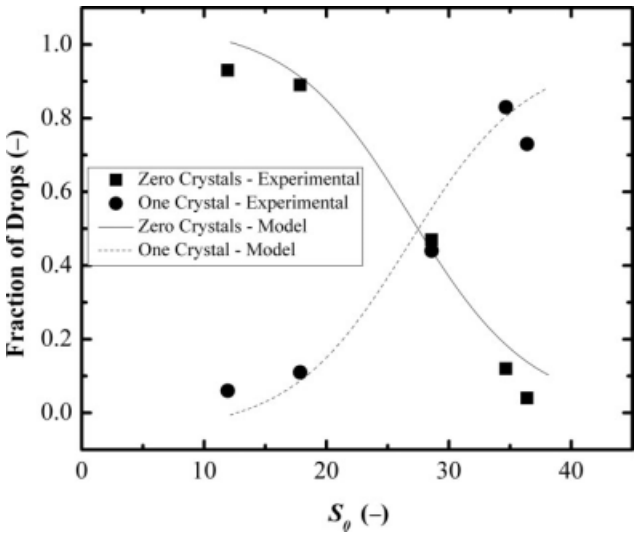

Figure 11. Fraction of drops containing lysozyme crystals after 72 h crystallization time in 150 μm drops.

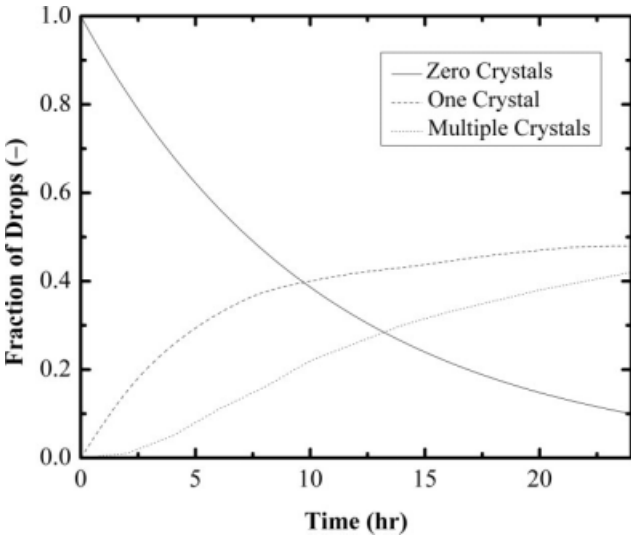

Figure 13. Distribution of the number of crystals per drop in 300 μm drops, S_0 = 3.1 at 298 K.

approximate the rapid growth limit. The microfluidic and multiwell experiments with lysozyme demonstrate how, with reliable growth and nucleation rate correlations, the relative growth and nucleation rate parameter $\ln(\tau_G/\tau_N)$ can be used to rapidly screen crystallization conditions for sets of conditions that will be expected produce a narrow CSD. However, the parameter $\ln(\tau_G/\tau_N)$ only describes the trajectory that crystallization process will follow. The solubility, nucleation thresholds and crystallization rate processes of different materials can vary over an extremely large range. Following the initial experimental screening of the parameter space, the Monte Carlo model may be used, for example, to design a second set of experiments to find a process where the nucleation time is reasonable and/or to determine the required crystallization time to meet a set of product CSD specifications.

Model-based process optimization: nonisothermal crystallization

The benefits of the model-based approach to designing a drop-based crystallization process become apparent when more complex operations are considered. One potential improvement to the drop-based crystallization process is a nonisothermal temperature profile similar to the approach used by Galkin and Vekilov; nucleation occurs during an initial low temperature, high supersaturation period followed by growth with no nucleation at a lower supersaturation. The cycle may then be repeated to nucleate crystals in additional

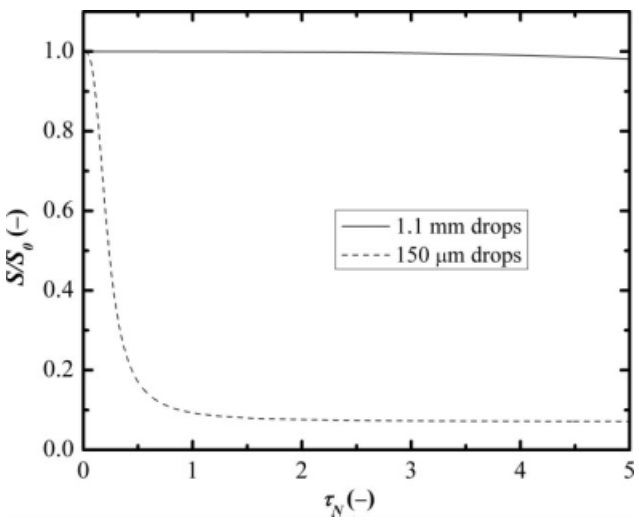

Figure 12. Predicted depletion of supersaturation due to the growth of a single lysozyme crystal in 1.1 mm drops where $\ln(\tau_G/\tau_N) = -2.9$ and in 150 μm drops where $\ln(\tau_G/\tau_N) = 3.8$.

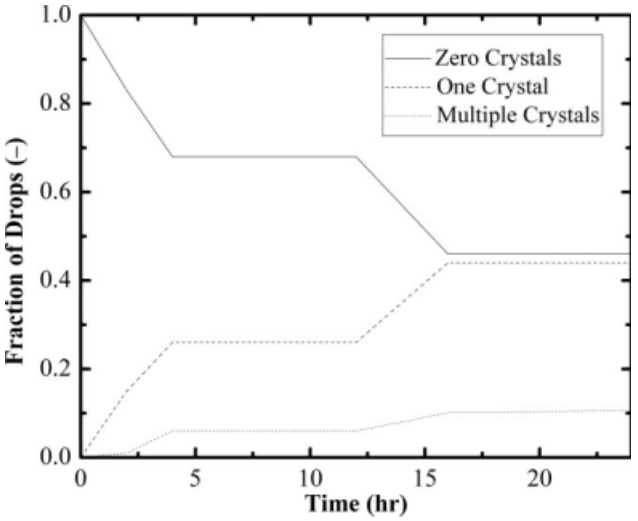

Figure 14. Distribution of the number of crystals per drop in 300 μm drops and S_0 = 3.1 with two alternating nucleation-growth cycles at 298 K and 313 K.

Table 4. Comparison of the CSD Produced from Isothermal Crystallization and the Nucleation-Growth Temperature Cycle

	Number Mean Crystal Size (μm)	CV	Fraction of Empty Drops	Fraction of Single Crystals	Fraction of Multiple Crystals
Isothermal crystallization	191	0.41	0.1	0.49	0.41
Nucleation-growth cycled	203	0.29	0.45	0.44	0.11

drops. To design an efficient, non-isothermal process the optimal times and temperatures of the nucleation and growth stages must be determined. Because of the increased number of parameters that must be optimized for the nonisothermal case, the traditional screening approach becomes tedious or impractical due to the large expansion of the matrix of screening experiments. The insight provided by the model developed in this paper can be used to streamline experimental design and process optimization by quickly identifying sets of conditions and/or non-isothermal temperature profiles that are likely to lead to the desired CSD. Experiments may then be targeted to test the most promising conditions as suggested by the model.

To illustrate potential benefits of the model-based optimization, simulations of the nucleation-growth temperature cycle were carried out for lactose in 300 μm drops with $\ln(\tau_G/\tau_N) = -0.4$ and $\tau_N = 2.4$ ($S_0 = 3.1$, 298 K, $t = 24$ h). Figure 13 shows the change in the number of crystals per drop as predicted by the Monte Carlo simulation. Figure 14 shows the model predictions with the same initial conditions using a non-isothermal temperature-time profile consisting of alternating 4 h nucleation periods at 298 K and 8 h growth periods at 313 K. The CSD statistics and fractions of drops with zero, one and multiple crystals are summarized in Table 4. The mean crystal size and fraction of drops with one crystal are similar for both the isothermal and nonisothermal temperature profiles. However, the nonisothermal profile reduces the fraction of drops containing multiple crystals by 73% and reduces the CV by 29% as compared with the isothermal case. The temperature-time profile identified earlier represents a potential improvement to the drop-based crystallization process for producing lactose crystals of controlled size. Work is ongoing to validate the effects of the proposed temperature profile and further optimize the drop-based lactose crystallization process by using the model predictions to direct experiments.

Conclusions

A mathematical model of crystallization in monodisperse drops was developed. The model includes many of the important crystallization phenomena that determine the number and size of crystals per drop, including stochastic primary nucleation and growth rate dispersion. By explicitly modeling these stochastic phenomena, the model is capable of predicting the distribution of the number of crystals per drop and the full crystal size distribution. The relative rates of crystal growth and nucleation, characterized by the dimensionless growth and nucleation time scales τ_N and τ_G, determine the results of the drop-based crystallization process. The dimensionless growth and nucleation time scales condense the effects of many process parameters into an intuitive form that may be used to predict the process outcome. The parameter $\ln(\tau_G/\tau_N)$ can be used to determine "at a glance" if a particular set of drop-based crystallization conditions is expected to yield a high fraction of drops with one crystal and a narrow CSD.

The model was validated with experimental data for lactose and lysozyme crystallization in drops. Using literature correlations for growth and nucleation rates, the model accurately predicted the experimentally observed crystallization behavior for a range of crystallization conditions. All of the model parameters have a physical basis and there are no fitted model parameters.

The identification of suitable crystallization conditions is the key challenge in the optimization of a drop-based crystallization process, whether it is for the production of a large quantity of crystals with controlled properties or the production of a single protein crystal for X-ray diffraction. The model development presented in this paper provides a framework for interpreting the results of drop-based crystallization experiments. Additionally, the model may be used as a predictive tool to aid experimental design to streamline the development of a process for producing drops containing single, high-quality crystals with the desired size.

Acknowledgments

The authors acknowledge the Australian Research Council and DuPont for funding, and acknowledge Emeritus Professor Ted White (University of Queensland) for useful discussions.

Notation

A_0 = Arrhenius pre-exponential factor (Nuclei m^{-3} s^{-1})
A = pre-exponential factor in classical nucleation theory (Nuclei m^{-3} s^{-1})
a = crystal growth order
CV = coefficient of variation
CV_G = coefficient of variation of crystal growth rate with GRD
d = drop size (m)
E_A = Arrhenius activation energy (J mol^{-1})
G = mean crystal growth rate (m s^{-1})
G_0 = initial crystal growth rate (m s^{-1})
J = nucleation rate (# m^{-3} s^{-1})
k = Boltzmann's constant (1.38×10^{-23} J K^{-1})
k_G = growth rate constant [m s^{-1} (concentration)$^{-n}$]
L_{max} = maximum crystal size in a drop (m)
L^* = dimensionless crystal size
m_{H_2O} = mass of water in a drop (kg)
m_{S0} = initial dissolved mass of solute in a drop (kg)
N_T = total number of drops
N_0 = number of drops with no crystals
N_1 = number of drops with one crystal
$N_{>1}$ = number of drops with more than one crystal
P_{Nuc} = probability of nucleation in one time step
p_j = probability of forming j crystals in a drop
S = supersaturation ratio
S_0 = initial supersaturation ratio
t = crystallization time (s)
t_{Growth} = characteristic growth time in a drop (s)
t_{Nuc} = characteristic nucleation time in a drop (s)

T = absolute temperature (K)
V = drop volume (m^3)
V_m = molecular volume (m^3)
$\mathbf{x}$ = vector of crystal size(s) in a drop (m)
%NaCl = NaCl concentration (wt %)

Greek letters

α_v = volume shape factor
γ = crystal-solution interfacial tension (mN m^{-1})
ΔC = absolute supersaturation (kg m^{-3} or g solute per 100 g water)
Δt = simulation time step (s)
ρ_C = crystal density (kg m^{-3})
σ = relative supersaturation
τ_G = dimensionless growth time in a drop
τ_N = dimensionless nucleation time in a drop

Literature Cited

1. Allen K, Davey RJ, Ferrari E, Towler C, Tiddy GJ, Jones MO, Pritchard RG. The crystallization of glycine polymorphs from emulsions, microemulsions, and lamellar phases. *Cryst Growth Des*. 2002;2:523–527.
2. Davey RJ, Hilton AM, Garside J. Crystallization from oil in water emulsions: particle synthesis and purification of molecular materials. *Chem Eng Res Des*. 1997;75:245–251.
3. Timsina MP, Martin GP, Marriott C, Ganderton D, Yianneskis M. Drug-delivery to the respiratory-tract using dry powder inhalers. *Int J Pharm*. 1994;101:1–13.
4. Mosharraf M, Nystrom C. The effect of particle-size and shape on the surface specific dissolution rate of microsized practically insoluble drugs. *Int J Pharm*. 1995;122:35–47.
5. Chayen NE. Comparative studies of protein crystallization by vapour-diffusion and microbatch techniques. *Acta Crystallogr D*. 1998;54:8–15.
6. Zheng B, Roach LS, Ismagilov RF. Screening of protein crystallization conditions on a microfluidic chip using nanoliter-size droplets. *J Am Chem Soc*. 2003;125:11170–11171.
7. Dombrowski RD, Litster JD, Wagner NJ, He Y. Crystallization of alpha-lactose monohydrate in a drop-based microfluidic crystallizer. *Chem Eng Sci*. 2007;62:4802–4810.
8. Anna SL, Bontoux N, Stone HA. Formation of dispersions using "flow focusing" in microchannels. *Appl Phys Lett*. 2003;82:364–366.
9. Srisa-nga S, Flood AE, White ET. The secondary nucleation threshold and crystal growth of alpha-glucose monohydrate in aqueous solution. *Cryst Growth Des*. 2006;6:795–801.
10. Berglund KA, Larson MA. Modeling of growth-rate dispersion of citric-acid monohydrate in continuous crystallizers. *AIChE J*. 1984; 30:280–287.
11. Klug DL, Pigford RL. The probability-distribution of growth-rates of anhydrous sodium-sulfate crystals. *Ind Eng Chem Res*. 1989;28: 1718–1725.
12. Garside J, Ristic RI. Growth-rate dispersion among adp crystals formed by primary nucleation. *J Cryst Growth*. 1983;61:215–220.
13. Kashchiev D, Kaneko N, Sato K. Kinetics of crystallization in polydisperse emulsions. *J Colloid Interface Sci*. 1998;208:167–177.
14. Feltham DL, Garside J. A mathematical model of crystallization in an emulsion. *J Chem Phys*. 2005;122:174910.
15. Vladisavljevic GT, Williams RA. Recent developments in manufacturing emulsions and particulate products using membranes. *Adv Colloid Interface*. 2005;113:1–20.
16. Sugiura S, Nakajima M, Tong JH, Nabetani H, Seki M. Preparation of monodispersed solid lipid microspheres using a microchannel emulsification technique. *J Colloid Interface Sci*. 2000;227: 95–103.
17. Galkin O, Vekilov PG. Direct determination of the nucleation rates of protein crystals. *J Phys Chem B*. 1999;103:10965–10971.
18. Baird JK. Theory of protein crystal nucleation and growth controlled by solvent evaporation. *J Cryst Growth*. 1999;204:553–562.
19. Mullin JW. *Crystallization*, 3rd ed. Oxford: Butterworth-Heinemann, 1993:527.
20. Lowe J, Ogden M, McKinnon A, Parkinson G. Crystal growth of sodium oxalate from aqueous solution. *J Cryst Growth*. 2002;237: 408–413.
21. Burton WK, Cabrera N, Frank FC. The growth of crystals and the equilibrium structure of their surfaces. *Philos Trans R Soc SA*. 1951;243:299–358.
22. Grimmett G, Stirzaker D. *Probability and Random Processes*. Oxford: Oxford University Press, 1982.
23. Liang B, Shi Y, Hartel RW. Growth-rate dispersion effects on lactose crystal size distributions from a continuous cooling crystallizer. *J Food Sci*. 1991;56:848–854.
24. McDonald EJ, Turcotte AL. Density and refractive indices of lactose solutions. *J Res Natl Bur Stand*. 1948;41:63–68.
25. Zheng B, Tice JD, Roach LS, Ismagilov RF. A droplet-based, composite PDMS/glass capillary microfluidic system for evaluating protein crystallization conditions by microbatch and vapor-diffusion methods with on-chip X-ray diffraction. *Angew Chem Int Ed*. 2004;43:2508–2511.
26. Shi D, Mhaskar P, El-Farra NH, Christofides PD. Predictive control of crystal size distribution in protein crystallization. *Nanotechnology*. 2005;16:S562–S574.
27. Durbin SD, Carlson WE. Lysozyme crystal-growth studied by atomic force microscopy. *J Cryst Growth*. 1992;122:71–79.
28. Forsythe E, Pusey ML. The effects of temperature and NaCl concentration on tetragonal lysozyme face growth-rates. *J Cryst Growth*. 1994;139:89–94.
29. Vekilov PG, Rosenberger F. Protein crystal growth under forced solution flow: experimental setup and general response of lysozyme. *J Cryst Growth*. 1998;186:251–261.
30. Cherdrungsi K. *Bulk Crystallization of Lysozyme*. University of Queensland: Brisbane, Queensland: Australia, 1999.
31. Zheng B, Tice JD, Ismagilov RF. Formation of arrayed droplets of soft lithography and two-phase fluid flow, and application in protein crystallization. *Adv Mater*. 2004;16:1365–1368.

Manuscript received Dec. 8, 2008, and revision received May 26, 2009.